The Nineth PSU Engineering Conference
MAY 2-3, 2011

Effect of self-contact on postbuckling behavior of variable-arc-length elastica

Boonchai Phungpaingam[1,*]
[1]Department of Civil Engineering, Faculty of Engineering, Rajamangala University of Technology Thanyaburi, Pathum-thani 12110
E-mail: phungpaigram_b@yahoo.com*

Abstract
This paper presents the effect of self-contact on postbuckling behavior of a variable-arc-length elastica where one end is clamped while the other end is placed on the sleeve joint. An axial force is applied at the sleeve end so that the elastica is well deflected into postbuckling state. The governing differential equations are established from equilibrium equations of a small segment of the elastica and geometric relations. The shooting method is employed as a tool for computing the numerical results. From the results, it reveals that the elastica subjected to the compressive load can lose its stability under some perturbation of displacement. Without the effect of self-contact, the elastica move through itself and the intersection points can be observed. By taking the self-contact into consideration, the elastica obeys the non-penetration condition and the elastica is stable again when it is deflected until the self-contact takes place.
Keywords: Variable-arc-length elastica, Stability, Self-contact

1. Introduction

The variable-arc-length (VAL) elastica is known as the elastica where one end can slide freely on the support. This causes the increase of the material into the system. This kind of model was pioneered by Chucheepsakul and Huang [1]. Afterwards, several papers about the VAL elastica were investigated by i) changing load case [2-6] and ii) changing boundary conditions [7]. However, the effect of self-contact was not included in their papers. Thus, for more practical results, the self-contact will be considered in this paper. It should be noted that the self-contact considered in this paper belongs to the class of rigid contact and the contact surface is assumed to be frictionless. This means the cross section of the elastica will not deform when self-contact occurs and no friction force at the interface. The concept of modeling the self-contact is to treat the contact force as a point load oriented normal to tangent vector at the contact point [8]. With this concept, the computation of the self-contact elastica is possible.

In this paper, the weightless VAL elastica of span length L and flexural rigidity EI is considered. One end of the elastica is completely fixed while the other end is placed on the sleeve support where the length can be increased by feeding the material at this support (see Fig. 1b). At a very large deflection, the each portion of the elastica can move to contact each other at a certain point. This is recognized as the self-contact elastica. The applications for this problem can be found in feeding systems (e.g., in printers, in rolling metal sheets, in conveyor belts, etc.) The governing differential equations for dealing with this problem are created from equilibrium of a small segment of the elastica together with the geometric relations. To explain the global behavior of the elastica, the system of the differential equations need to be integrated and the end values must be according with the boundary conditions of the problem. This constitutes the two-point boundary values problem where the shooting method is an efficient tool for this kind of problems. Hence, the shooting method is employed in this study.

From the results, it is found that the VAL elastica can lose its stability for some perturbation of displacement. The instability of the elastica can be ceased by considering the self-contact of the elastica.

2. Statement of the problem

In Fig. 1, undeformed and deformed configurations of the elastica are demonstrated. In undeformed state, the weightless elastica is rested on the rigid surface (see Fig. 1a). This can be viewed as a feeding system operated by rolling balls at left and right ends. If the roller at the left end is not in function and the rolling system at the right end tries to push the material into the system, this results in a compressive force applied at the right end. Under the compressive force, the elastica can be deflected into Fig. 1b. As can be observed that during the deflection the span length L of the elastica does not change but the total arc-length is increased where this characteristic can be considered as the VAL elastica.

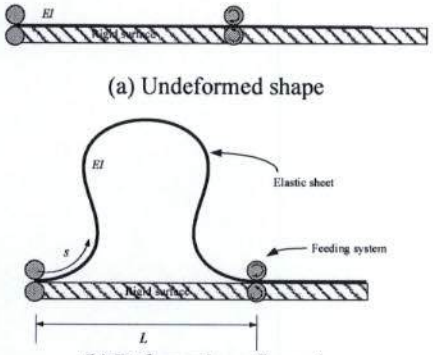

Figure 1. Undeformed and deformed configurations: (a) undeformed configuration; (b) deformed configuration

3. Formulations

By considering a weightless elastica and its small segment in Fig. 2, the equilibrium equations can be expressed by

$$\frac{dN}{ds}=0;\frac{dV}{ds}=0;\frac{dM}{ds}=-V\frac{dx}{ds}+N\frac{dy}{ds} \qquad \text{(1a-c)}$$

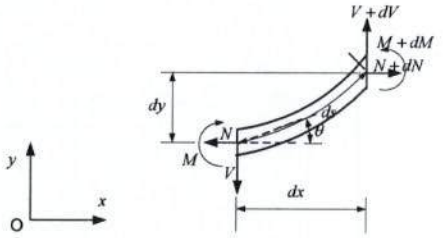

Figure 2. An elastica segment

N,V and M are normal force, shear force and bending moment, respectively. s is arc-length of the elastica. The geometric relations can be given by

$$\frac{dx}{ds}=\cos\theta;\frac{dy}{ds}=\sin\theta \qquad \text{(2a,b)}$$

x and y are horizontal and vertical distances measured from the reference point O. θ is an angle of the elastica defined from the x-axis.

For the sake of the generality, the following non-dimensional parameters are introduced.

$$\bar{N}=\frac{NL^2}{EI};\bar{V}=\frac{VL^2}{EI};\bar{M}=\frac{ML}{EI} \qquad \text{(3a-c)}$$

$$\bar{x}=\frac{x}{L};\bar{y}=\frac{y}{L};\bar{s}=\frac{s}{L} \qquad \text{(3d-f)}$$

Subsequently, equations 1 and 2 can be rewritten into non-dimensional forms as

$$\frac{d\bar{N}}{d\bar{s}}=0;\frac{d\bar{V}}{d\bar{s}}=0;\frac{d\bar{M}}{d\bar{s}}=-\bar{V}\cos\theta+\bar{N}\sin\theta \qquad \text{(4a-c)}$$

$$\frac{d\bar{x}}{d\bar{s}}=\cos\theta;\frac{d\bar{y}}{d\bar{s}}=\sin\theta \qquad \text{(4d,e)}$$

Equation 4 forms a set of the non-linear governing differential equations of the system defined in a very small region $d\bar{s}$. To describe the whole system of the elastica, Eq (4) must be integrated. There are several techniques of integration such as elliptic integral technique [2,4,5,7] and numerical integration by Runge-Kutta algorithm [6]. The finite element method was also used as a numerical tool for solving this kind of problems [1,3,6]. In this paper, the numerical integration (i.e., Runge-Kutta method) is employed. The integration is performed from one end to the other end of the elastica and this is referred to the two-point boundary value problem where the shooting method can be served as a powerful tool for calculating the results. The boundary conditions of the problem are as follows

At $\bar{s}=0$:

$$\bar{x}(0)=0;\bar{y}(0)=0;\theta(0)=0 \qquad \text{(5a-c)}$$

At $\bar{s}=\bar{s}_t$:

$$\bar{x}(\bar{s}_t)-1=0;\bar{y}(\bar{s}_t)=0;\theta(\bar{s}_t)=0 \qquad \text{(5d-f)}$$

$\bar{s}_t$ is the total arc-length of the elastica. As can be seen in Eq 4, there are three unknown parameters (i.e., $\bar{N}(0),\bar{V}(0),\bar{M}(0)$. Therefore, three constraint equations need to be supplied (i.e., Eqs (5d-f)). By integrating Eqs (4a-e) associating with boundary conditions in Eqs (5a-f), the solution of contact-free VAL elastica can be obtained.

For the case of the self-contact elastica, there are two additional unknown parameters increased from the contact-free elastica. They are the arc-length at a contact point $\bar{s}_c$ and the contact force at that point $\bar{F}_c$. Thus, it is necessary to increase the constraint equations from 3 equations (the contact-free case) into 5 equations (the self-contact case). Since the deflection of the elastica is symmetry, the additional constraint equations are utilized the advantage of symmetry conditions of the deflection. The constraint equations are

$$\theta(\bar{s}_c)-\frac{\pi}{2}=0;\bar{x}(\bar{s}_c)-0.5=0 \qquad \text{(6a,b)}$$

Furthermore, the elastica in this case is divided into three segments: i) $\bar{s}=0\rightarrow\bar{s}_c$, ii) $\bar{s}=\bar{s}_c\rightarrow\bar{s}_t-\bar{s}_c$ and iii) $\bar{s}=\bar{s}_t-\bar{s}_c\rightarrow\bar{s}_t$. This is because there is a

discontinuity (jump) in force $\bar{N}$ at the contact point. Thus, the integration of the entire length of the elastica is also divided into three parts as previous mention. The continuity of bending moment and displacements at the contact point is considered during the integration process as well as the discontinuity of the force $\bar{N}$ at the contact point.

4. Results and discussion

4.1 Contact-free elastica

In this case, the self-contact is not taken into account. The load-deflection curve is presented in Fig. 3.

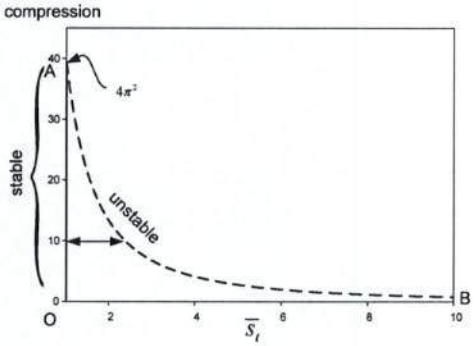

Figure 3. Load-deflection curve for contact-free VAL elastica.

From the curve, the naturally straight elastica is buckled at $\|\bar{N}\|_{cr} = 4\pi^2$. Afterwards, it loses the stability where the stiffness of the system becomes negative (i.e., negative slope of load-deflection curve). At a given load that less than the critical load $\|\bar{N}\| < \|\bar{N}\|_{cr}$, there are two equilibrium configurations. One is stable configuration (i.e., straight configuration) and the other is unstable configuration (i.e., deformed configuration). This means that, under compression $\|\bar{N}\| < \|\bar{N}\|_{cr}$, the system can lose its stability when the straight elastica (line OA) is disturbed so that it snaps into the broken line of the equilibrium path (line AB) in Fig. 3. For $\|\bar{N}\| > \|\bar{N}\|_{cr}$, the system is definitely unstable. Under some small perturbation, the system will lose its stability. The equilibrium configurations are plotted in Fig. 4.

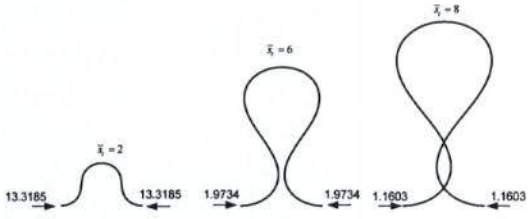

Figure 4. Equilibrium configurations of the VAL elastica (the contact-free case)

As can be seen that, the elastica moves through itself when the self-contact is not taken into account for total arc-length $\bar{s}_t = 8$. By varying total arc-length, it is found that the self-contact of the elastica begins at total arc-length $\bar{s}_t = 6.61$ (see Fig. 5).

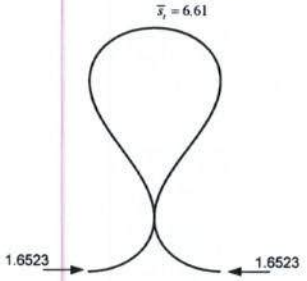

Figure 5. Equilibrium configuration for $\bar{s}_t = 6.61$

4.2 Self-contact elastica

In the case of self-contact elastica, the load-deflection curve is shown in Fig. 6. From Fig. 6, we can observe that the equilibrium path emanated from point C is the equilibrium path for the elastica where self-contact takes place.

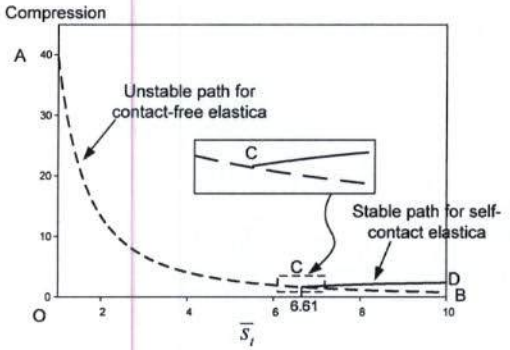

Figure 6. Load-deflection curve for self-contact elastica

As can be observed that the equilibrium path for self-contact elastica (i.e., the solid line after point C) is stable path since the stiffness of the system becomes positive (i.e., load increases as deflection increases). The equilibrium shapes of the self-contact elastica are illustrated in Fig. 7.

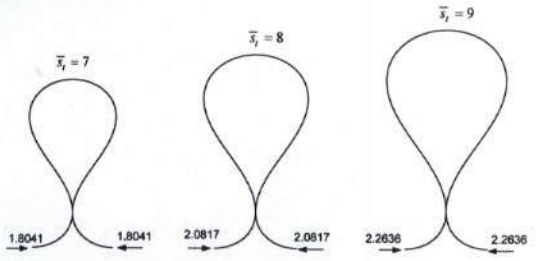

Figure 7. Equilibrium configurations for self-contact elastica

5. Simple experiment

In this section, a simple experiment was setup to validate the theoretical results with experimental results. The experiment was conducted to compare the geometry (maximum height, $\bar{h}_{\max} = \frac{h_{\max}}{L}$) from the analytical results and experimental results. The maximum height $\bar{h}_{\max}$ can be computed by integrating Eq (4e) from $\bar{s} = 0$ to $\bar{s} = \frac{\bar{s}_t}{2}$. Figure 8 shows an elastic sheet (i.e., the polycarbonate sheet) in the experiment and the maximum height $h_{\max}$.

Since the material model is assumed to be linearly elastic material, the highly flexible material is necessary. In this experiment, a polycarbonate sheet is utilized as the elastic sheet. The span length L of the elastic sheet is assigned to be 30 cm. Since the material length is limited to around 100 cm, with span length of 30 cm. the total arc-length $\bar{s}_t$ cannot be larger than 3 (90 cm.).

In the analysis, it indicates that the system is unstable and any measurement during unstable state is very difficult because only a small disturbance causes the system into motion. Thus, in this experiment, the elastica needs to be stabilized by preventing the both ends from motion (clamped at the both ends). After stabilization of the system, the height of the elastica can be read easily by image processing.

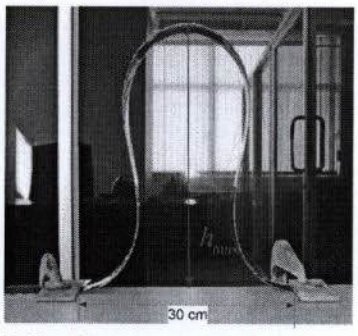

Figure 8. Simple experiment to scale the maximum height (in the figure $\bar{s}_t = 3$)

Table1 The maximum height of the elastica: theoretical results

$\bar{s}_t$	$\bar{h}_{\max}$	$h_{\max}(cm.)$
2	0.74661	22.3983
3	1.19161	35.7483

Table2 The maximum height of the elastica: experimental results and theoretical results

$\bar{s}_t$	$h_{\max}(cm.)$	
	Theory	Experiment
2	22.3983	22.9070
3	35.7483	36.3855

In table 1, the maximum height from the theoretical results is presented. In table 2, the theoretical results and experimental results are compared. It can be seen that both results are in good agreement. Unfortunately, the material length is limited. The experiment for higher values of total arc-length $\bar{s}_t$ does not conduct in this paper. However, in the further study, it is interesting to setup more advanced experiment such as setting the load cell to read the axial force and using a very long polycarbonate sheet to observe the effect of self-contact in the experiment.

6. Conclusion

The variable-arc-length elastica where one end is clamped and the other end is placed on the sleeve joint is investigated. The analytical results are in good agreement with those from the experimental results. From the results, it can be concluded that without effect of self-contact, the elastica can lose its stability by some perturbation of displacement. The elastica can gain the stability again if it moves to contact itself.

References

[1] Chucheepsakul, S. and Huang, T. 1992. Finite Element Solution of Large Deflection Analysis of a Class of Beam. Proceeding of the Computational Method in Engineering. 1: 45-50.

[2] Chucheepsakul, S., Buncharoen, S. and Wang, C.M. 1994. Large Deflection of Beams under Moment Gradient. Journal of Engineering Mechanics (ASCE), 120:1848-1860.

[3] Chucheepsakul, S. and Huang, T. 1997. Finite Element Solution of Variable-arc-length Beams under a Point Load. Journal of Engineering Mechanics (ASCE), 123:968-970.

[4] Chucheepsakul, S., Wang, C.M., He, X.Q. and Monprapussorn, T. 1999. Double Curvature Bending of Variable-arc-length Elasticas. Journal of Applied Mechanics (ASME), 66:87-94.

[5] Chucheepsakul, S. and Phungpaingam, B. 2004. Elliptic Integral Solutions of Variable-arc-length Elastica under an Inclined Follower Force, Zeitschrift fur Angewandte Mathematik und Mechanik (ZAMM), 84: 29-38.

[6] Athisakul, C. and Chucheepsakul, S. 2008. Effect of Inclination on Bending of Variable-arc-length Beams Subjected to Uniform Self-Weight. Engineering Structures, 30: 902-908.

[7] Zhang, X. and Yang, J. 2005. Inverse Problem Elastica of a Variable-arc-length Beam Subjected to a Concentrated Load. Acta Mechanica Sinica, 21: 444-450.

[8] Flaherty, J.E. and Keller, J.B. 1973. Contact Problem Involving a Buckled Elastica. Journal of Applied Mathematics (SIAM), 24: 215-225.